Using volumetric optical coherence tomography to achieve spatially resolved organ of Corti vibration measurements

Brian L. Frost, Clark Elliott Strimbu and Elizabeth S. Olson

Citation: The Journal of the Acoustical Society of America **151**, 1115 (2022); doi: 10.1121/10.0009576
View online: https://doi.org/10.1121/10.0009576
View Table of Contents: https://asa.scitation.org/toc/jas/151/2
Published by the Acoustical Society of America

JASA ARTICLE

Using volumetric optical coherence tomography to achieve spatially resolved organ of Corti vibration measurements

Brian L. Frost,[1,a)] Clark Elliott Strimbu,[2] and Elizabeth S. Olson[2,3]

[1]*Department of Electrical Engineering, Columbia University, 500 W. 120th St., Mudd 1310, New York, New York 1002, USA*

[2]*Department of Otolaryngology Head and Neck Surgery, Vagelos College of Physicians and Surgeons, Columbia University, 630 W. 168th St., New York, New York 10032, USA*

[3]*Department Biomedical Engineering, Columbia University, 351 Engineering Terrace, 1210 Amsterdam Ave., New York, New York 10027, USA*

ABSTRACT:

Optical coherence tomography (OCT) has become a powerful tool for measuring vibrations within the organ of Corti complex (OCC) in cochlear mechanics experiments. However, the one-dimensional nature of OCT measurements, combined with experimental and anatomical constraints, make these data ambiguous: Both the relative positions of measured structures and their orientation relative to the direction of measured vibrations are not known *a priori*. We present a method by which these measurement features can be determined via the use of a volumetric OCT scan to determine the relationship between the imaging/measurement axes and the canonical anatomical axes. We provide evidence that the method is functional by replicating previously measured radial vibration patterns of the basilar membrane (BM). We used the method to compare outer hair cell and BM vibration phase in the same anatomical cross section (but different optical cross sections), and found that outer hair cell region vibrations lead those of the BM across the entire measured frequency range. In contrast, a phase lead is only present at low frequencies in measurements taken within a single optical cross section. Relative phase is critical to the workings of the cochlea, and these results emphasize the importance of anatomically oriented measurement and analysis.

 https://doi.org/10.1121/10.0009576

(Received 23 October 2021; revised 3 January 2022; accepted 26 January 2022; published online 16 February 2022)

[Editor: Sunil Puria] Pages: 1115–1124

I. INTRODUCTION

Optical coherence tomography (OCT) is an imaging modality capable of imaging and nanometer-scale vibrometry at a depth into a sample.[1,2] An OCT image is formed of axial scans, or *A-scans*, which are one-dimensional maps of sample reflectivity recorded at each depth along the optical axis. The A-scan is generated from raw photodetector data via a Fourier transform and contains both a magnitude (corresponding to A-scan intensity, which forms the image) and a phase. Several A-scans can be taken along a line segment perpendicular to the optical axis to form a two-dimensional brightness scan, or *B-scan*, and several B-scans can in turn be taken along the axis perpendicular to these two directions to form a volume scan.

For vibrometry purposes, a series of A-scans taken over time at the same position is referred to as a motion scan, or *M-scan*. The phase of a pixel value as a function of time is proportional to the subpixel displacement of the structures within that pixel.[2] More specifically, it is proportional to the *projection* of the total three-dimensional motion of the structure onto the beam direction, or optical axis; i.e., OCT performs one-dimensional vibrometry.

In applications in physiology, the direction of the optical axis is usually chosen on the basis of experimental and anatomical constraints. The result is that B-scans are often far off from the canonical anatomical cross sections seen in the literature. As M-scans provide a projection of the three-dimensional motion onto the optical axis, it is essential to be able to relate the optical axis to more familiar anatomical axes. Volume scans contain all the information necessary to determine the orientation of the optical axis relative to the local anatomy. We are interested in finding the relationship between local anatomical coordinates and the optical coordinates of the OCT system. Mathematically, this problem can be framed as one of changing bases, a coordinate transformation.

We focus on cochlear mechanics research, wherein OCT is used for both imaging and vibrometry.[3–9] The sensory tissue of the cochlea is composed of the cellular organ of Corti and the acellular structures of the basilar membrane (BM) and tectorial membrane (TM), which together form the organ of Corti complex (OCC), as shown in Fig. 1(c). Until recently, simultaneous vibration measurements of different structures within the OCC were not possible, as standard techniques such as laser Doppler vibrometry were not capable of measuring at a depth into a sample. OCT has allowed for intra-OCC measurements, which have revealed motions that are characteristically different from BM

[a)]Authors to whom correspondence should be addressed: b.frost@columbia.edu and eao2004@cumc.columbia.edu

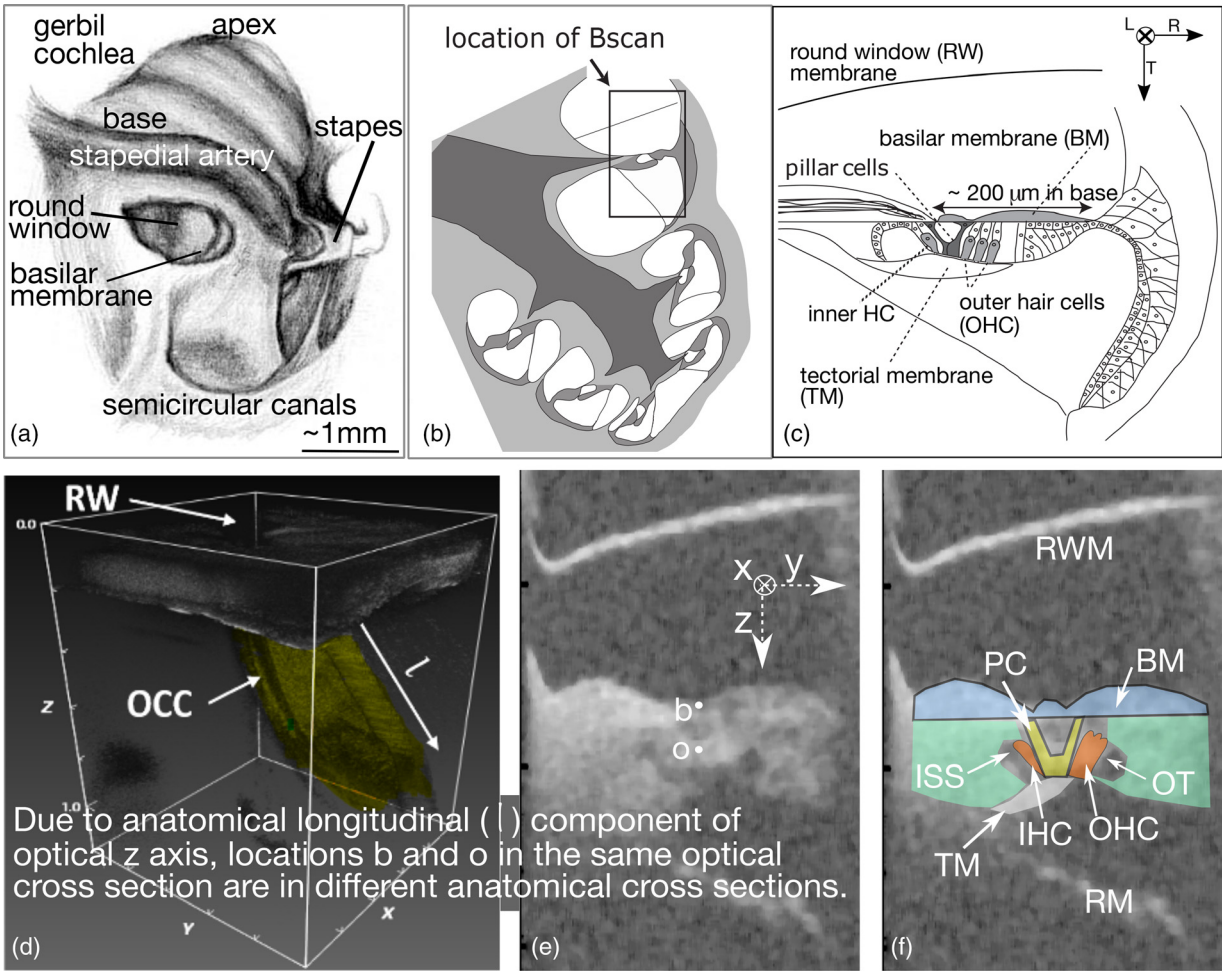

FIG. 1. (Color online) (a) Experimental view of the gerbil cochlea (drawing by V. Cervantes). (b) Cross-sectional diagram of the snail-shaped cochlea showing the region of imaging, which is accessed through the RW at the top. The dark gray region indicates the auditory nerve. The auditory neurons branch out to contact the sensory tissue (medium gray region), which spirals within the fluid-filled (white region), bone-encased (light gray region) cochlea. (c) Diagram of an idealized cochlear cross section positioned in the anatomical coordinate system. (d) Representative OCT volume scan (x × y × z size = 1 mm × 1 mm × 1.38 mm) of the gerbil cochlea taken through the RW membrane. The sensory tissue (OCC) is the gold band spiraling from base to apex, away from the RW. The longitudinal direction **l** is labeled. (e) B-scan with two dots identifying the BM (labeled b) and the OHC region (labeled o). From the path of the OCC in the volume scan, it is seen that the z axis has a component in the longitudinal direction so that b and o in the same B-scan lie in different anatomical cross sections. (f) Labeled B-scan. IHC, inner hair cell; ISS, internal spiral sulcus (fluid space); OT, outer tunnel; PC, pillar cell; RM, Reissner's membrane; RWM, round window membrane.

motion. Of particular interest are the electromotile outer hair cells (OHCs) involved in cochlear amplification. The micromechanics of the cochlear amplifier—the active process in the cochlea that is responsible for the boosting of vibrations at lower sound pressure levels (SPLs)—are still not well understood, but OCT has made it possible to probe these mechanics in a more direct way. However, the uniaxial nature of vibrometry, including OCT vibrometry, leads to important ambiguities in the data. Without an understanding of the cochlea's orientation in each experiment, comparisons between experiments, as well as comparisons between experiments and models, cannot reasonably be made, imposing a barrier to the interpretation of cochlear mechanics results. This barrier can be overcome by making measurements from several viewing angles, but this is only rarely possible in in vivo experiments in the cochlea.[8,9]

In a standard experiment, a B-scan is used to orient the experimenter within the cochlea, and one A-scan within this B-scan is selected for vibration measurements. We call these the *orienting B-scan* and *measurement A-scan*, respectively. The component of vibration in the direction of the optical axis is detected at each pixel in the measurement A-scan. The several-micrometer axial resolution (~8 μm optical resolution, 2.7 μm pixel size) of the Thorlabs Telesto 311C OCT, along with the known anatomy, allows us to localize regions that correspond to structures in the OCC [Figs. 1(c), 1(e), and 1(f)].

The OCC spirals around the cochlea in what is referred to as the *longitudinal* direction (positive from base to apex). At a given cross section with fixed longitudinal position, the direction into and out of the OCC [vertical in Fig. 1(c)] is the *transverse* direction, and the direction across the OCC is the *radial* direction [horizontal in Fig. 1(c)]. Along the spiral, these anatomical coordinates vary in orientation with respect to fixed spatial coordinates.

Figure 1(c) gives the standard view of a cochlear cross section (referred to from here on as the *anatomical cross*

https://doi.org/10.1121/10.0009576

section), and in past work, we have interpreted our orienting B-scans [Figs. 1(e) and 1(f)] with respect to this view. In fact, because of experimental constraints, the optical axis usually has substantial components in all three anatomical directions, meaning that our B-scans are not images of anatomical cross sections. Figure 1(d) shows a volume scan of the gerbil cochlea through the round window (RW), with the OCC visible as a gold band spiraling downward from the RW at the top of the volume. The z axis has a significant longitudinal component, signifying that a y,z cross section of this volume will not be as in Fig. 1(c), in which the longitudinal direction is perpendicular to the cross section. Thus, although the BM and OHC structures can be measured in the same B-scan, they actually lie in different anatomical cross sections [Figs. 1(d) and 1(e)].

We developed a program that uses experimenter input to form a planar approximation of the BM and using this, derives the coordinate transformation that relates the optical coordinate system to the anatomical coordinate system. The coordinate transformation allows us to achieve two objectives: (1) to express the axial direction, and thus the direction of motion recorded in the A-scan, in terms of the anatomical components, and (2) to describe the positions of all structures within a volume scan in either optical or anatomical coordinates. In particular, we can determine how far along the longitudinal axis the measured OHC region is from the measured BM. We find that in A-scans from our motion measurements in gerbil, the measured OHCs are often $>40\,\mu$m apical of the measured BM, a significant distance given that an OHC is $10\,\mu$m in diameter and that $40\,\mu$m is a large enough distance to see differences in the phase and magnitude of the cochlear traveling wave.[10] We used the coordinate transformation to create a graphical user interface (GUI) program that allows the user to explore a volume scan in either anatomical or optical coordinates. With this program, the experimenter can determine the location to take an A-scan to capture the motion at a specific anatomical position, allowing experimenters to measure BM and OHC motion at the same anatomical cross section. We provide evidence that the program is functional by using known properties of BM vibration patterns.

Although the present work focuses on measurements in the cochlea, the method can be applied to any problem in which a locally planar structure (i.e., a surface with a large radius of curvature compared with the size of the imaged region) is present, such as the retina.

II. METHODS

A. Locally planar model

The BM is a surface-like structure that spirals around the cochlea. The first-order (linear) approximation to a smooth surface at some point **p** is a plane, which is analogous to the approximation of a smooth curve at a point as a line.

We model the BM as a plane near the point at which we take vibration measurements. A plane is defined by three noncolinear points, **A**, **B**, and **C** (Fig. 2). Three points along the BM within a single B-scan would be colinear, so we must select points within at least two B-scans to define the plane. One natural choice is to take several parallel B-scans, or a volume scan, and choose points within two different B-scans in this volume. Two factors affect the validity of the planar approximation: The BM has nonzero curvature and

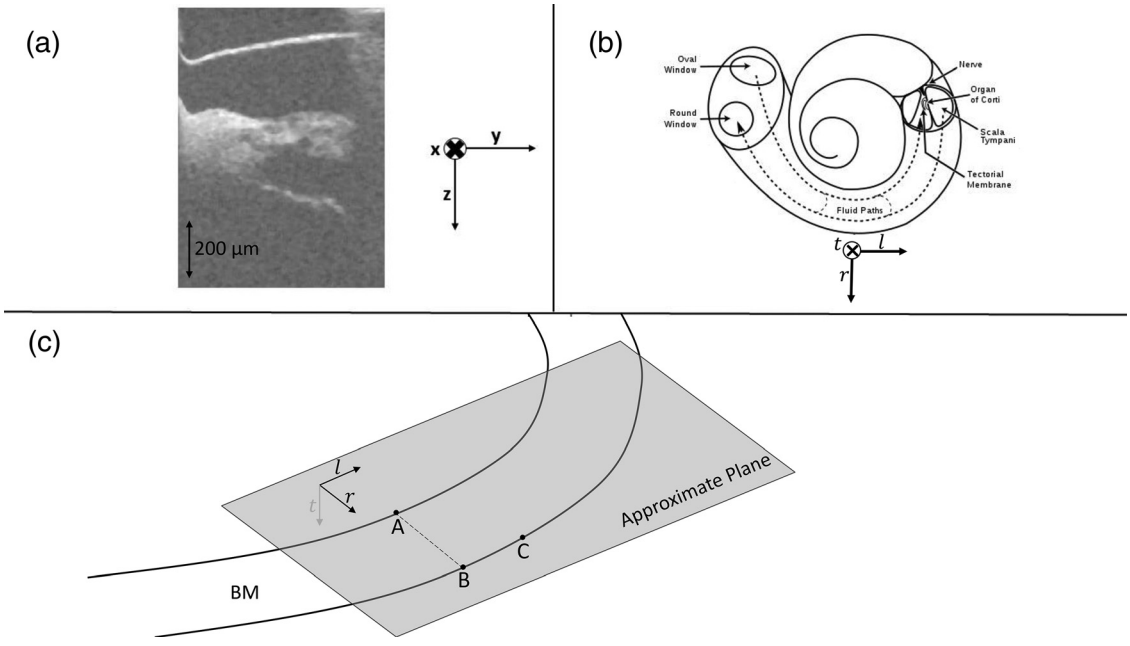

FIG. 2. The coordinate systems used in the development of this program. (a) The optical coordinate system, defined with respect to the orienting B-scan, shown alongside a representative B-scan. (b) The anatomical coordinate frame, which varies so as to always be tangent to the BM at any point, shown at a point along a diagram of the cochlea. (c) The local approximation of the anatomical coordinate system, defined with respect to a plane that approximates the BM's plane (shown as a gray surface).

has deviations from flatness because of its anatomical structure. Increasing the distance between each of the three selected points decreases the accuracy of the approximation due to the curvature of the surface but helps to ensure that small-scale variations that interfere with smoothness do not distort the planar estimation. We also choose plane-defining points that avoid the substructure within the BM; in particular, we choose points along the radial edges of the BM, not within its arched center. (On the side of the BM facing the organ of Corti, the BM runs straight between its radial edges, but in gerbil, on the side facing the scala tympani, the BM has an arched shape.[11] We use the straight side of the BM to define the plane. The arched anatomy is not present in most other mammals.)

B. Coordinate systems

A B-scan that includes the OCC was taken to provide initial positioning. We refer to this imaging plane as the *orienting B-scan*. The *optical coordinate system* is defined with respect to this plane as follows: The direction into the sample (the optical axis) is **z**. This is the vertical direction in the B-scan, which is positive from top to bottom. The horizontal direction in the B-scan from left to right is **y**, and the normal to the orienting B-scan is the **x** direction such that $\mathbf{x} \times \mathbf{y} = \mathbf{z}$ [Fig. 1(e)]. That is, **x** is in the direction into the page. The volume scan is generated by taking multiple **y,z** plane B-scans along the x axis, with the orienting B-scan as the center scan within the volume.

The *anatomical coordinate frame* is defined in the following way: The direction along the tonotopic axis (the direction along which the cochlea spirals) from base to apex is the longitudinal axis **l**, the direction across the BM normal to **l** from the modiolus to the outer wall is the radial axis **r**, and the direction normal to the BM toward the scala media is the transverse axis $\mathbf{t} = \mathbf{l} \times \mathbf{r}$ [Fig. 2(b)]. This frame varies smoothly in orientation with respect to Cartesian coordinates as it spirals along the cochlea. Our goal is to approximate these anatomical coordinates in terms of optical coordinates at all locations where we wish to measure vibrations. We do this using the planar approximation of the BM local to the orienting B-scan, as described above. The normal to the BM plane is the local transverse direction **t**, and the longitudinal and radial directions lie within the plane defined by the local BM. Figure 2 shows these coordinate systems, as well as a local approximation of anatomical coordinates.

C. Determining the approximate anatomical plane

A volume scan is acquired using ThorImage software from Thorlabs, which allows the user to select the dimensions of the volume (which is always in the shape of a rectangular prism), as well as the spacing between the A-scans, which comprise the volume. In selecting the spacing, it is important to choose a spacing well below the lateral resolution of the OCT system so that as few as possible features are lost as a result of quantization. Our lateral resolution is $\sim 10\,\mu$m, so we use 2-μm $\times$ 2-μm spacing. The axial spacing is determined by the bandwidth and wavelength of the light source, and is 2.7 μm.[1] This volume is then imported into our coordinate transformation program. The volume scan is selected so that the orienting B-scan lies in the center, where the volume comprises a set of B-scans parallel to this orienting B-scan. As described in Sec. II A, at least two B-scans are necessary to select points that define the local BM plane. So that the approximation is best near the orienting B-scan, we choose two parallel B-scans separated by Δx in the **x** direction, equidistant from the orienting B-scan. In the first of these B-scans, we select two points on the BM, **A** and **B**. We select **B** to be the point on the BM nearest the outer wall and **A** to be the point nearest the spiral lamina. The BM in this cross section should be well approximated by the line segment $\overline{\mathbf{BA}}$. (A video demonstrating these and subsequent steps is included as supplementary material.[12])

We select the third point **C** to be a point on the BM closest to the outer wall in the second B-scan. We choose the second B-scan to be apical to the orienting B-scan (or mathematically, the projection of **l** onto $\overline{\mathbf{BC}}$ is positive). Because these three points determine the plane, we know the plane's unit normal vector:

$$\mathbf{t} = \frac{(\mathbf{A} - \mathbf{B}) \times (\mathbf{C} - \mathbf{B})}{||(\mathbf{A} - \mathbf{B}) \times (\mathbf{C} - \mathbf{B})||}.$$

This vector **t** is the transverse unit vector, the normal to the BM. We go on to find the longitudinal and radial vectors **l** and **r**. We selected both **B** and **C** to be points on the BM nearest to the outer wall so that they lie at the same transverse and radial positions in two different anatomical cross sections. Thereby, the vector

$$\mathbf{l} = \frac{\mathbf{C} - \mathbf{B}}{||\mathbf{C} - \mathbf{B}||}$$

is the local approximation of the longitudinal direction. To complete the right-handed coordinate system, the radial direction is given by

$$\mathbf{r} = \mathbf{t} \times \mathbf{l}.$$

Following this analysis, the anatomical coordinate vectors $\mathbf{r}, \mathbf{t}, \mathbf{l}$ are represented in the ordered basis of optical coordinates $\{\mathbf{x}, \mathbf{y}, \mathbf{z}\}$. The **z** components of the anatomical coordinate vectors l_z, r_z, and t_z give the z axis (optical axis, the direction of measurement), written in anatomical coordinates, and their relative sizes indicate the degree to which a given anatomical direction is represented in a measurement.

D. Determining the coordinate transformation

To proceed, our goal is to find the relationship between optical and anatomical coordinates. Now that we have represented the anatomical coordinates in a system that is stationary with respect to optical coordinates, this can be framed as a change-of-basis problem. A mapping between two

https://doi.org/10.1121/10.0009576

coordinate systems is described by a unique change-of-basis matrix U. The process described in Sec. II C produces the anatomical coordinate vectors $\{\mathbf{l},\mathbf{r},\mathbf{t}\}$ in terms of optical coordinates. The mapping *from anatomical to optical coordinates* is the 3×3 matrix, whose columns are the anatomical coordinate vectors written in optical coordinates, i.e.,

$$U=\begin{pmatrix} l_x & r_x & t_x \\ l_y & r_y & t_y \\ l_z & r_z & t_z \end{pmatrix}.$$

To explore the volume in anatomical coordinates, we map *from optical to anatomical coordinates*. This is the inverse mapping of U. As all change-of-basis matrices are unitary, $U^{-1}=U^{\mathrm{T}}$ maps from optical to anatomical coordinates.

E. Determining the displacement measurement direction

Our first goal is to determine the direction of the vibratory motion we are measuring in anatomical coordinates. We refer to the displacement measurements along the optical ($\mathbf{z}$) axis as $d(\mathbf{p},f)$. This is a scalar-valued function of the position $\mathbf{p}$ and the frequency of the stimulus f. $d(\mathbf{p},f)$ is the $\mathbf{z}$ projection of the three-dimensional displacement $\mathbf{D}(\mathbf{p},f)$. We can write $\mathbf{D}(\mathbf{p},f)$ in the space of anatomical coordinates as follows:

$$\mathbf{D}(\mathbf{p},f)=D_l(\mathbf{p},f)\mathbf{l}+D_r(\mathbf{p},f)\mathbf{r}+D_t(\mathbf{p},f)\mathbf{t}.$$

As we have expressed the unit vectors $\mathbf{l}$, $\mathbf{r}$, and $\mathbf{t}$ in the optical coordinates in Sec. II D, we know the $\mathbf{z}$ components of these unit vectors, which we write as l_z, r_z, and t_z respectively. As such, our measurement is given by

$$d(\mathbf{p},f)=D_l(\mathbf{p},f)l_z+D_r(\mathbf{p},f)r_z+D_t(\mathbf{p},f)t_z.$$

In practice, l_z, r_z, and t_z are often all nonnegligible, and with a unidirectional motion measurement, we cannot determine D_l, D_r, and D_t separately. [For clarity, consider the alternative: If we were able to choose the optical axis to be perpendicular to the local plane of the BM, l_z and r_z would equal 0, and t_z would equal 1, so $d(\mathbf{p},f)=D_t(\mathbf{p},f)$.]

F. Exploring optical space in anatomical coordinates

The change-of-basis matrix U gives us a simple way to explore the volume scan in terms of optical and anatomical coordinates simultaneously. We have developed a GUI, which is based in MATLAB and available upon request, that allows the user to traverse the volume in either coordinate system, as shown in Fig. 3. We refer to the GUI program as the *orienting GUI*. As the user moves about the volume in one coordinate system, the other set of coordinates is computed by applying either U or U^T for anatomical-to-optical or optical-to-anatomical transformations, respectively. The red line represents the projection of the plane onto the B-scan. Users can use sliders or enter values to traverse the volume in either coordinate system and see

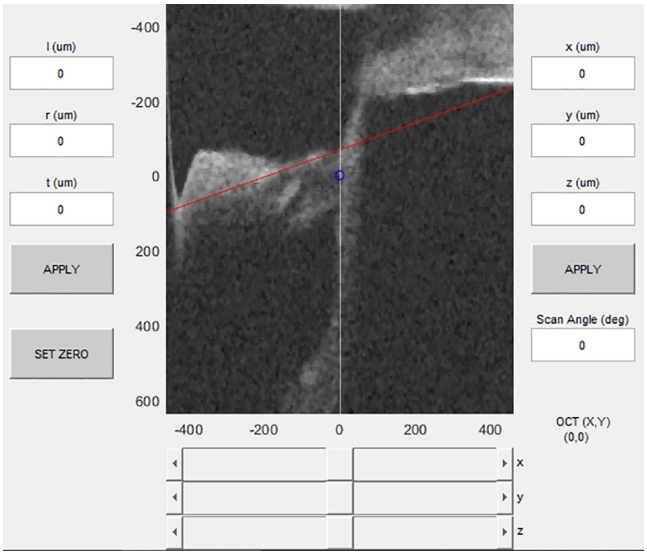

FIG. 3. (Color online) GUI used to explore volumes in both optical and anatomical coordinates. Shown is the orienting B-scan from gerbil experiment 900. The coordinate values of the blue point's location are shown in the anatomical (left) and optical (right) systems, and the A-scan in which this point lies is shown in white. The red line is the planar approximation of the BM projected onto the displayed B-scan.

the corresponding coordinates in both systems (anatomical on the left, optical on the right).

The orienting GUI has two main purposes: (1) to find the anatomical locations of structures measured in one A-scan and (2) to pick locations for measurement (in optical coordinates) based on their anatomical locations. One important application is to measure vibrations of different structures (e.g., the BM and OHC) within the same anatomical cross section (i.e., same $\mathbf{l}$ coordinate value). This is achieved as follows: First, observe an A-scan in which both the BM and the OHC are present; second, use the orienting GUI to determine the longitudinal location of the OHCs relative to the BM in that A-scan; third, determine the optical coordinates of a position on the BM in the same anatomical cross section as those OHCs; and finally, use the OCT positioning mirrors to set the optical axis along each of these A-scans sequentially and take motion measurements at each. This process allows the measurement of the motion of OHCs and BM within the same anatomical cross section.

It is important to note that structures within the OCC have tilts in longitudinal directions, so measuring a part of a cell in the same longitudinal cross section as the BM does not mean that the *entire* cell lies in the same longitudinal cross section. However, the tilt of gerbil OHCs in the longitudinal direction is small ($\sim 5^\circ$), so anatomical tilt has no significant effect on the application explored in the present work.[13] Other structures in the OCC (in particular, the Deiters' cell processes) have a significant longitudinal tilt that should be accounted for when their motion is measured.

G. Sensitivity to point selection

We close this section by considering the sensitivity of our model to the choice of points **A**, **B**, and **C** to understand

how variation in user input will affect the operation of our program. To explore this problem, we consider a particular volume scan from gerbil experiment 903 and a corresponding planar approximation based on experimenter-selected points **A**, **B**, and **C**. In determining these points, we used a 20-μm spacing between B-scans. We consider the case in which two of these points are fixed and the third is selected at some point within a 40-μm $\times$ 40-μm square of the originally selected point [Figs. 4(a) and 4(c)]. To contextualize this square, the lateral resolution of our OCT device is $\sim$10 μm, and axial resolution is $\sim$8 μm, which means that the square of tested values is $\sim 4 \times 5$ units of optical resolution. Then, we consider the transverse unit vector computed by using this newly selected point and compute the angle it makes with the original unit transverse vector via the cosine rule of dot products. We do this by varying point **A** with **B** and **C** fixed and again by varying point **C** with **A** and **B** fixed. The two tested squares of points are shown in Figs. 4(a) and 4(c). Figures 4(b) and 4(d) show the resulting variation in the angle of the transverse unit vector relative to the originally computed angle.

The planar approximation is more sensitive to choice in the point **C** than the point **A**. This is unsurprising, as point **A** is far from both points **B** and **C**, whereas point **C** is quite close to **B**. The largest variation is $\sim$15°, with point **C** chosen at the very edge of the test box, two units of lateral resolution and two and a half units of axial resolution away from the originally selected point. Next, we explore the effect of this angular variation to the orienting GUI described in Sec. III F (i.e., the program to locate OHCs and BM in the same longitudinal cross section). For this application, we start with a point at the OHCs and then move purely in the computed transverse direction until we reach the BM. This distance is usually $\sim$45 μm. The angular variation noted above, with maximum 15 degrees (termed θ), gives rise to a variation in distance that is calculated using the law of cosines:

$$d_{BM} = 45\sqrt{2 - 2\cos\theta}.$$

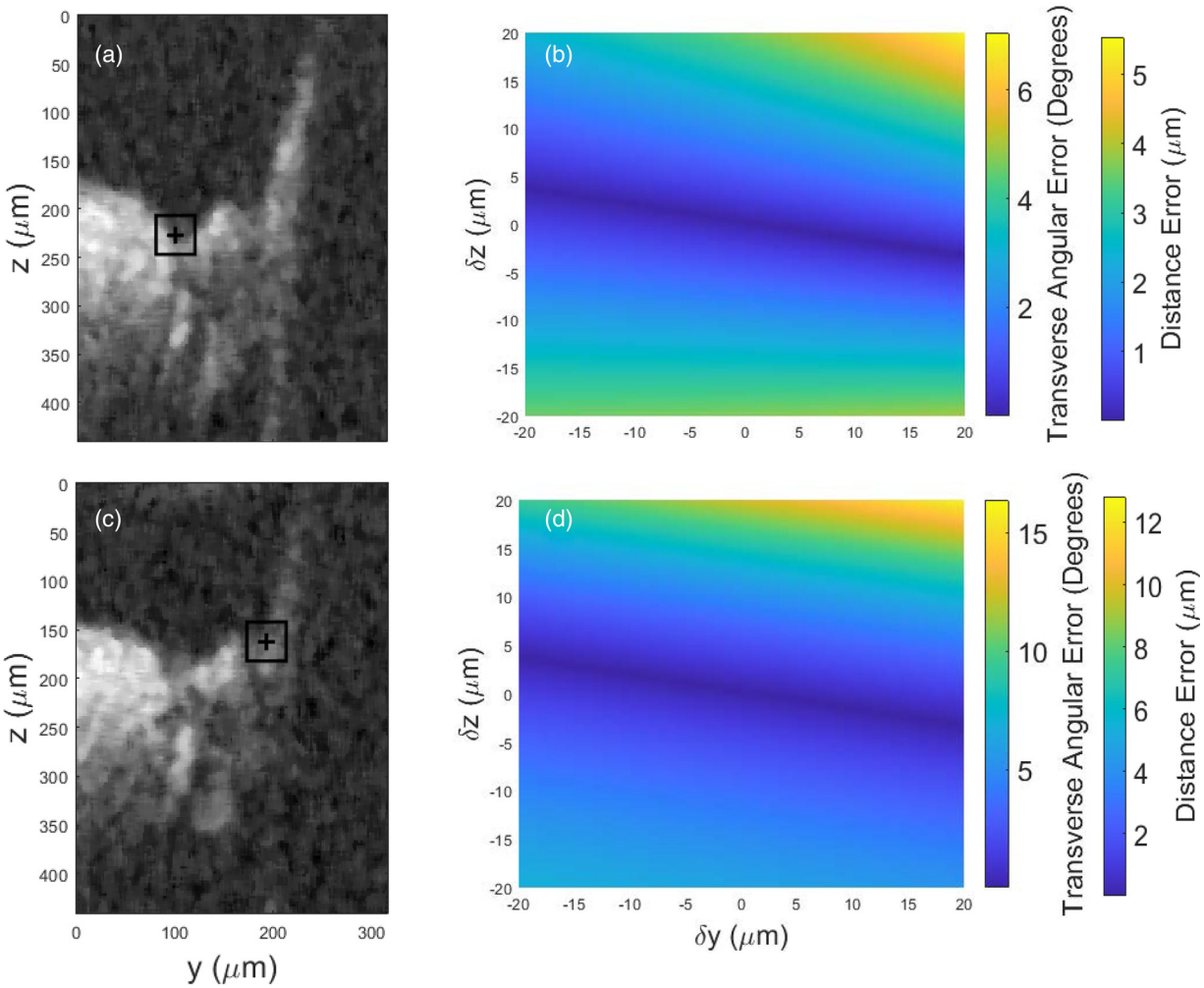

FIG. 4. (Color online) (a) A zoomed-in B-scan of the OCC in gerbil experiment 903, wherein points **A** and **B** are chosen. The experimenter's guess for point **A** is marked as a black cross, and the 40-μm $\times$ 40-μm box of tested **A** values is shown centered around this point. (b) Angular difference between transverse unit vectors computed using the experimenter-chosen points and points in the box shown in (a) with points **B** and **C** fixed. The corresponding distance between computed BM positions is shown in a separate color bar to the right. (c) Similar to (a), but in the second B-scan in which **C** is chosen with the tested values of **C** shown. (d) Similar to (b), but using different values of **C** and fixing points **A** and **B**.

https://doi.org/10.1121/10.0009576

The distance variation computed from the angular variation is shown as a second color bar in Figs. 4(b) and 4(d). (Note that this calculation corresponds to a displacement vector containing components in all three anatomical directions and, thus, is an upper bound on the variation in the longitudinal distance, which is the variation important for our particular application.) A worst-case distance variation of 12 μm is in the far upper-right corner of Fig. 4(d). Within the more reasonable selection range of 20 μm × 20 μm about the selected point, we see a maximum variation of ∼5 μm. This variation can be compared with the ∼40-μm longitudinal distance between OHCs and the BM within a single B-scan noted in Sec. I. Using 5 μm as the maximum variability with reasonably careful point selection, the use of the program to locate OHCs and BM in the same longitudinal cross section will be accurate to ∼12%.

III. RESULTS

A. Representative example

We began with a 1-mm × 1-mm × 1.38-mm volume scan from gerbil through the round window. All data were taken using the Thorlabs Telesto 311C OCT system using the LSM03 objective lens. We used B-scans $\Delta x = 20$ μm apart (each 10 μm from the orienting B-scan) to choose points **A**, **B**, and **C**, as shown in Fig. 5. With these three points, we determined the anatomical coordinates **l**, **r**, and **t**. This also allows us to find the displacement measurement breakdown: $d(\mathbf{p},f) = D_l(\mathbf{p},f)l_z + D_r(\mathbf{p},f)r_z + D_t(\mathbf{p},f)t_z$. The uniaxial measurement does not allow us to determine D_l, D_r, and D_t, but it shows which of these anatomical motions our uniaxial measurement is most sensitive to. In our example, with a commonly used angle of approach through the round window, the component multipliers had values $l_z = 0.8$, $r_z = -0.1$, and $t_z = 0.6$, showing that in this example, the most represented anatomical component of motion was longitudinal, with significant representation in the transverse direction. The value of r_z was relatively small, meaning that the optical axis is nearly perpendicular to the radial axis, and thus, a motion measurement along this optical axis is not very sensitive to radial vibration.

Next, we used the orienting GUI to find the anatomical positions of the BM and OHC region along the initial A-scan, as shown in Figs. 6(a) and 6(b). We found that the OHCs in the initial A-scan lay ∼45 μm apical from the BM. We then used the program to determine the optical coordinates of the BM 45 μm apical of the initial A-scan; this is a point on the BM in the same anatomical cross section as the OHCs in the initial A-scan [Fig. 6(c)]. We took vibration measurements along these two A-scans in two sequential data runs, using the quantitative output of the orienting GUI to position the OCT mirrors to access each A-scan in turn. This process can also be seen in the video included as supplementary material.[12]

Figure 6(d) shows the vibration phases of the BM and OHC region from two A-scan locations in the same animal: Run 1 OHC and BM are in the same A-scan, whereas run 2 BM is in the same anatomical cross section as run 1 OHC. The BM and OHC vibration phases can be compared as measured along one A-scan (red compared with dark blue) or as measured within a single anatomical cross section (red compared with light blue). Comparisons within an A-scan show that the OHC vibration phase led the BM significantly at low frequencies, with the lead diminishing to zero as frequency increased. On the other hand, comparisons within the anatomical cross section show that OHC vibration led the BM over the entire frequency range. The difference in the BM vibration measurements in the two runs likely occurs because of the longitudinal progression of the phase of the cochlea's traveling wave, which is frequency dependent. In these results, the OHC–BM phase differences within one A-scan deviated from the OHC–BM phase differences within an anatomical cross section by as much as a quarter-cycle. In the analysis of cochlear mechanics, a quarter-cycle phase "error" could shift an interpretation of results from power neutral to power generating or power absorbing. Thus, this magnitude of potential phase reporting error significantly affects the study of the operation of the cochlea and the cochlear amplifier.[5,9,14]

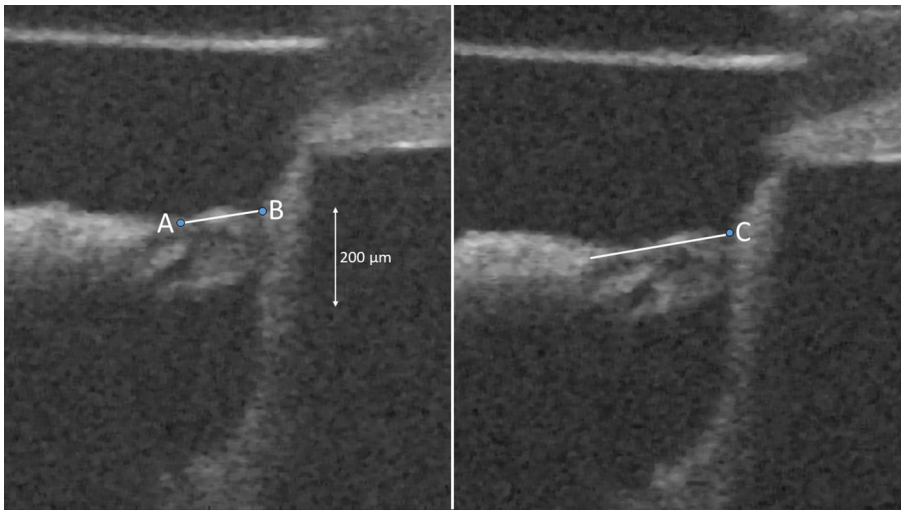

FIG. 5. (Color online) Plane approximation process, gerbil experiment 900. Two B-scans from a single volume scan, 20 μm apart. Points **A** and **B** are chosen in the first B-scan (left). This determines the line segment (shown in white) that approximates the BM in this cross section. In the second B-scan (right), **C** is chosen, completely defining the plane. The projection of that plane onto the second B-scan is shown in white.

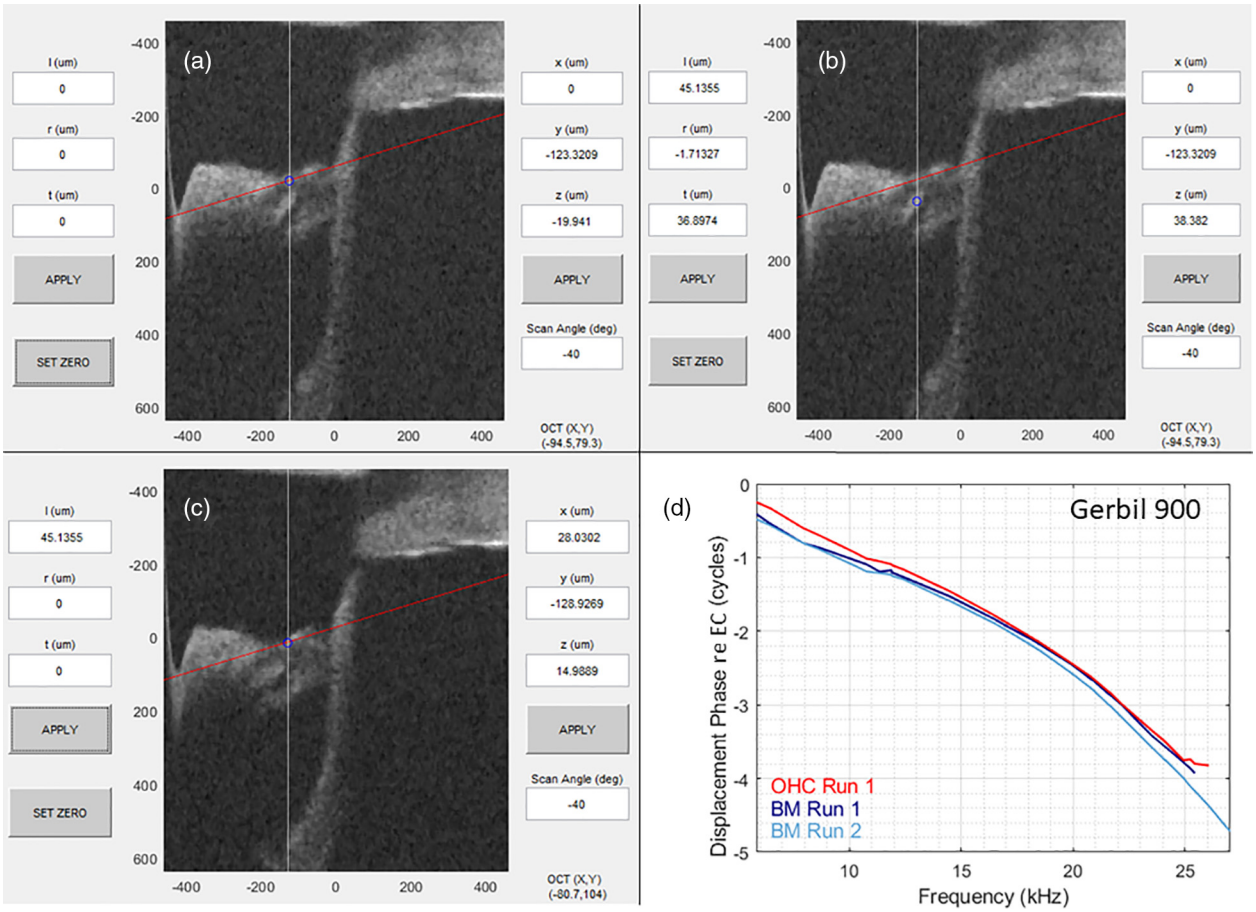

FIG. 6. (Color online) Use of the orienting GUI to measure BM and OHC in the same anatomical cross section. (a) To begin, we select an A-scan containing BM and OHC. The zero point is set to be on the BM along this A-scan, as shown here. (b) We move the z slider so that the blue point is on the OHCs and the A-scan has not changed. Only the z optical coordinate changes, whereas all three anatomical coordinates have changed. The l value indicates that the OHCs are $\sim$45 μm apical of the BM in this A-scan. (c) We find the measurement location necessary to measure BM motion in the same cross section as OHC from the previous A-scan by moving to the point with the same l position but with $r = t = 0$. The OCT(x,y) coordinates on the bottom right are the output data we use to direct the OCT positioning mirrors to the desired A-scan location. (d) We display the measured displacement phase with respect to ear canal (re EC) at the OHC and BM in the first A-scan as well as the BM in the second A-scan. The OHC from run 1 and BM from run 2 are in the same anatomical cross section. Data taken at 80-dB SPL.

B. Testing against known physiology

To test the functionality of our method, we used data from an in vivo gerbil experiment in which our program was used to probe an established property of cochlear mechanics. It is known that at a given longitudinal position (anatomical cross section), the phase of BM motion is approximately the same at all locations spanning the BM radially.[15,16] We used the BM planar approximation and coordinate transformation (the orienting GUI) to take BM motion recordings at what

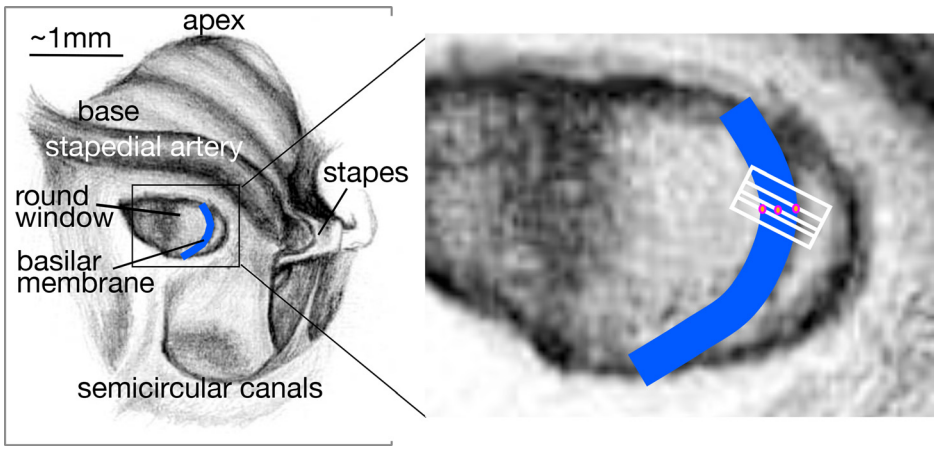

FIG. 7. (Color online) Illustration of the method used to test the operation of the orienting GUI against known physiology. The blue band in each view indicates the basilar membrane. The magenta dots in the expanded view on the right indicate points that span the BM radially. The white box is the **x,y** plane of a volume scan, with the interior white lines indicating the y axis of the B-scans in which the magenta points lie. The orienting GUI identifies the locations of the magenta points, all of which lie in different B-scans.

https://doi.org/10.1121/10.0009576

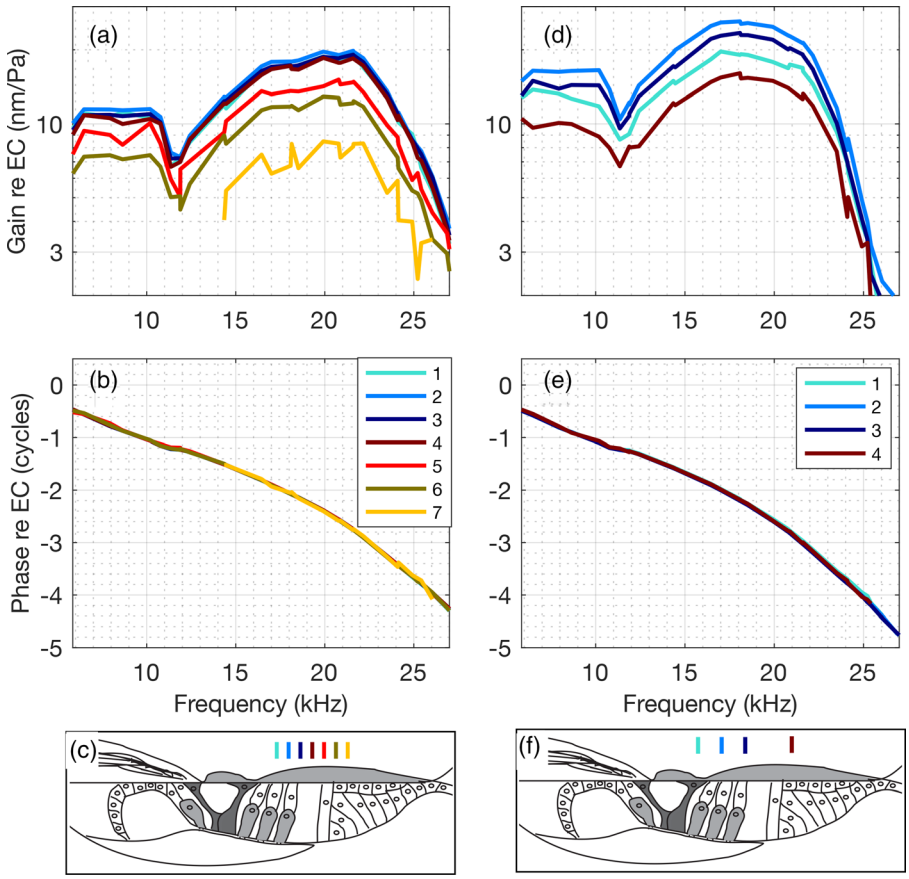

FIG. 8. (Color online) BM displacement data from gerbil experiment 900 from two different head angles provide evidence that the GUI orientation program correctly identified the anatomical radial axis. (a)–(c) BM displacement amplitude and phase taken along a single anatomical cross section at seven radial locations spaced 10 μm apart medial (aqua) to lateral (yellow), with locations approximated in (c). (d)–(f) BM displacement amplitude and phase taken in a different anatomical cross section at radial locations spaced 20 μm or 40 μm apart medial (aqua) to lateral (brown), with locations approximated in (f). Data taken at 80-dB SPL. re EC, with respect to ear canal.

we computed to be locations that were all at the same longitudinal position, locations that spanned the BM radially. We performed this process within two volume scans, each taken at a different orientation of the gerbil's head with respect to the scanner. The volume scans were taken such that a single B-scan was not perpendicular to the longitudinal axis; thus, orienting across the BM radially involved navigating through a series of B-scans. Figure 7 illustrates the concept, with the boxed region indicating the x,y plane of the volume scan. In the results shown in Fig. 8, the vibration phase did not change as the measurement location moved radially across the BM. Thus, our results confirm established findings, indicating that the orienting GUI successfully identified the anatomical cross section.

IV. CONCLUSIONS

We have presented a method for determining the location and orientation of the structures in OCT volume scans relative to their canonical anatomical coordinates. This method requires the presence of a locally planar structure, and the experimenter's selection of three points within two parallel B-scans. It is a simple and fast process by which to add meaning to OCT measurements. In the context of cochlear mechanics, we now can determine the components of motion that are represented in our vibration measurements. This program also allows us to measure structures with certain anatomical relationships to one another, such as being in the same anatomical cross section, despite not lying in the same B-scan. Being able to take measurements of different structures at the same anatomical cross section allows for more direct motion comparisons to be made. We have shown that this corrects for traveling wave phase differences between structures in a single A-scan. The method can be used to probe phase differences among OHCs, Hensen's cells, and the BM, furthering the detailed mapping of micromechanical motions and the understanding of cochlear operation.

Although three-dimensional motion of the OCC can never be determined through a one-dimensional measurement, this program nevertheless offers insight into the results of three-dimensional cochlear models. When it is known which axis measurements are taken, model results along this same axis can be compared with OCT measurements. In future work, measurements of the same structure taken at two or three known angles could be used to reconstruct two- or three-dimensional motion.

[1]J. A. Izatt and M. A. Choma, *Theory of Optical Coherence Tomography* (Springer Berlin Heidelberg, Berlin, Heidelberg, 2008), pp. 47–72.
[2]M. A. Choma, A. K. Ellerbee, C. Yang, T. L. Creazzo, and J. A. Izatt, "Spectral-domain phase microscopy," Opt. Lett. **30**(10), 1162–1164 (2005).
[3]S. S. Gao, R. Wang, P. D. Raphael, Y. Moayedi, A. K. Groves, J. Zuo, B. E. Applegate, and J. S. Oghalai, "Vibration of the organ of Corti within the cochlear apex in mice," J. Neurophysiol. **112**(5), 1192–1204 (2014).
[4]W. Dong, A. Xia, P. D. Raphael, S. Puria, B. E. Applegate, and J. S. Oghalai, "Organ of Corti vibration within the intact gerbil cochlea measured by volumetric optical coherence tomography and vibrometry," J. Neurophysiol. **120**(6), 2847–2857 (2018).

[5]E. Fallah, C. E. Strimbu, and E. S. Olson, "Nonlinearity and amplification in cochlear responses to single and multi-tone stimuli," Hearing Res. **377**, 271–281 (2019).
[6]C. E. Strimbu, Y. Wang, and E. S. Olson, "Manipulation of the endocochlear potential reveals two distinct types of cochlear nonlinearity," Biophys. J. **119**(10), 2087–2101 (2020).
[7]F. Chen, D. Zha, A. Fridberger, J. Zheng, N. Choudhury, S. L. Jacques, R. K. Wang, X. Shi, and A. L. Nuttall, "A differentially amplified motion in the ear for near-threshold sound detection," Nat. Neurosci. **14**(6), 770–774 (2011).
[8]H. Y. Lee, P. D. Raphael, A. Xia, J. Kim, N. Grillet, B. E. Applegate, A. K. E. Bowden, and J. S. Oghalai, "Two-dimensional cochlear micromechanics measured in vivo demonstrate radial tuning within the mouse organ of Corti," J. Neurosci. **36**(31), 8160–8173 (2016).
[9]N. P. Cooper, A. Vavakou, and M. Van Der Heijden, "Vibration hotspots reveal longitudinal funneling of sound-evoked motion in the mammalian cochlea," Nat. Commun. **9**(1), 1–12 (2018).
[10]T. Ren, "Longitudinal pattern of basilar membrane vibration in the sensitive cochlea," Proc. Nat. Acad. Sci. USA **99**(26), 17101–17106 (2002).
[11]S. Kapuria, C. R. Steele, and S. Puria, "Unraveling the mystery of hearing in gerbil and other rodents with an arch-beam model of the basilar membrane," Sci. Rep. **7**(1), 1–10 (2017).
[12]See the supplementary material at https://www.scitation.org/doi/suppl/10.1121/10.0009576 for a video of the method of determining the approximate anatomical plane.
[13]Y.-J. Yoon, C. R. Steele, and S. Puria, "Feed-forward and feed-backward amplification model from cochlear cytoarchitecture: An interspecies comparison," Biophys. J. **100**(1), 1–10 (2011).
[14]W. Dong and E. S. Olson, "Detection of cochlear amplification and its activation," Biophys. J. **105**(4), 1067–1078 (2013).
[15]N. P. Cooper, "Radial variation in the vibrations of the cochlear partition," in *Recent Developments in Auditory Mechanics*, edited by H. Wada, T. Takasaka, K. Ikeda, K. Ohyama, and T. Koike (World Scientific, Singapore, 2000), pp. 109–115.
[16]R. L. Warren, S. Ramamoorthy, N. Ciganović, Y. Zhang, T. M. Wilson, T. Petrie, R. K. Wang, S. L. Jacques, T. Reichenbach, A. L. Nuttall, and A. Fridberger, "Minimal basilar membrane motion in low-frequency hearing," Proc. Nat. Acad. Sci. USA **113**(30), E4304–E4310 (2016).